ELSEVIER

Thin Solid Films 379 (2000) 188–194

thin solid films

www.elsevier.com/locate/tsf

Effect of added ionic salt on the quantum efficiency of self-assembled films prepared with poly(*p*-phenylene vinylene)

Jinhan Cho[a], Kookheon Char[a,*], Sun-Young Kim[a], Jong-Dal Hong[b], Sung Kyun Lee[c], Dong Young Kim[d]

[a]*School of Chemical Engnieering, Seoul National University, San 56-1, Shinlim-dong, Kwanak-gu, Seoul 151-742, South Korea*
[b]*Department of Chemistry, University of Inchon, Dowha-dong, Namgu, Inchon 402-749, South Korea*
[c]*Department of Chemistry, Hanyang University, 17 Haendang-dong, Seoul 133-791, South Korea*
[d]*Polymer Materials Lab, Korea Institute of Science and Technology, P.O. Box 131, Cheongryang, Seoul 130-650, South Korea*

Received 9 February 2000; received in revised form 12 July 2000; accepted 31 August 2000

Abstract

Multilayer electroluminescence (EL) devices based on the self-assembled layers of poly(*p*-phenylene vinylene) (PPV) and poly(sodium 4-styrenesulfonate) (PSS) were prepared and characterized. The increase of recombination region for the radiative decay of polaron excitons in the film device was achieved by two different fabrication methods: increase of the number of bilayers and increase of ionic strength of PSS solution using a salt additive. When simply increasing the number of bilayers, the relative device efficiency was improved proportional to the number of bilayers deposited. In contrast, the addition of NaCl salt to the PSS dipping solution resulted in higher thickness deposition but exhibited low luminescence level as well as low quantum efficiency. We believe that the decrease of the quantum efficiency, despite the increased thickness in the case of added salt in the PSS solution, is caused by the defect formation at the interface between PPV/PSS film and Al electrode. In order to minimize this problem, we inserted one insulating bilayer composed of cationic poly(allylamine hydrochloride) (PAH) and anionic poly(methacrylic acid) (PMA) in direct contact with the Al electrode. Upon this insertion, significant improvement of device efficiency was achieved and the quantum efficiency was shown to be proportional to the total film thickness even in the case of the salt addition scheme.

Keywords: Electrical properties and measurements; Electronic devices; Organic semiconductors; Surface defects

1. Introduction

There is recently great interest in using semiconducting electroluminescent polymers for the fabrication of light-emitting devices (LED). From numerous studies reported to date on the polymer LEDs, polymer/electrode interfaces play important roles, though still poorly understood, in determining the operating characteristics and the stability of the devices [1,2]. Although organic LEDs with high quantum efficiency and brightness have been successfully fabricated with spin-coated polymer films, much room is still left for the improvement of these devices and more complete understanding of device characteristics is necessary. A detailed understanding of these interfaces will open up novel ways to fabricate such improved organic devices.

Recently, a layer-by-layer self-assembly method based on the electrostatic attraction between opposite charges has been implemented in the LED fabrication. It was shown that this method could easily control the film

* Corresponding author. Tel.: +82-2-880-7431; fax: +82-2-888-7295.
E-mail address: khchar@plaza.snu.ac.kr (K. Char).

0040-6090/00/$ - see front matter
PII: S0040-6090(00)01555-8

thickness at a molecular level and allow one to insert desired heterogeneous layers in the organic thin film structure [3–5]. It also contributes to the better understanding of roles of the heterogeneous layers for the charge injection at interfaces between organic layers and electrodes as well as for the effect of film thickness on recombination zone (i.e. film thickness for polaron excitons created through the recombination of holes and electrons).

In this work, we have investigated the operating characteristics of electroluminescence (EL) devices composed of alternating poly(*p*-phenylene vinylene) (PPV) and poly(sodium 4-styrenesulfonate) (PSS) films. These multilayer devices were prepared using the self-assembly technique by expanding the concept of conjugation length control in the self-assembled films reported previously [6,7]. Two different fabrication methods to increase the recombination region were tested: one is to simply increase the number of bilayers and the other is by the increase of ionic strength of PSS solution using a salt additive. The change of quantum efficiency of the self-assembled EL devices prepared by the two different methods as well as the cause of the change was studied.

2. Experimental section

2.1. Materials

PPV precursor was prepared by polymerization of a bis-sulphonium salt of *p*-xylene using the method given by Lenz et al. [8]. The reaction product was dialyzed with a molecular weight cut-off at 12 000 and the concentration of PPV precursor in aqueous solution was estimated by gravimetry to be 0.013 M. Poly(sodium 4-styrenesulfonate) (PSS) (Aldrich, $M_W = 70\,000$), poly(allylamine hydrochloride) (PAH) (Aldrich, $M_n = 50\,000 \sim 65\,000$) and poly(methacrylic acid) (PMA) (Polyscience, $M_w = 15\,000$) were diluted to 0.01 M and used without further purification. The pH was adjusted to 3.3 by adding HCl.

2.2. Buildup of multilayer

Positively charged PPV precursor was initially deposited onto the negatively charged substrate as described previously [6,7]. Ultrapure water (with a resistivity of 18 MΩ cm) obtained from an ion-exchange and filtration unit (Milli-Q, Millipore GmbH) was used for all the experiments and cleaning steps. Substrates used for all the adsorption experiments were quartz glasses of size 25 mm × 50 mm.

The quartz substrates were cleaned by sonication in a hot mixture of H_2SO_4/H_2O_2 (7:3) for 3 h. The substrates were then heated in a mixture of $H_2O/H_2O_2/NH_3$ (5:1:1) to 80°C for 1 h, and subsequently dried with nitrogen gas to obtain substrates with negatively charged surface. The substrates were subsequently immersed alternately in the PPV precursor solution and in the PSS solution for 20 min for each deposition. Both solution concentrations were fixed at 0.01 M.

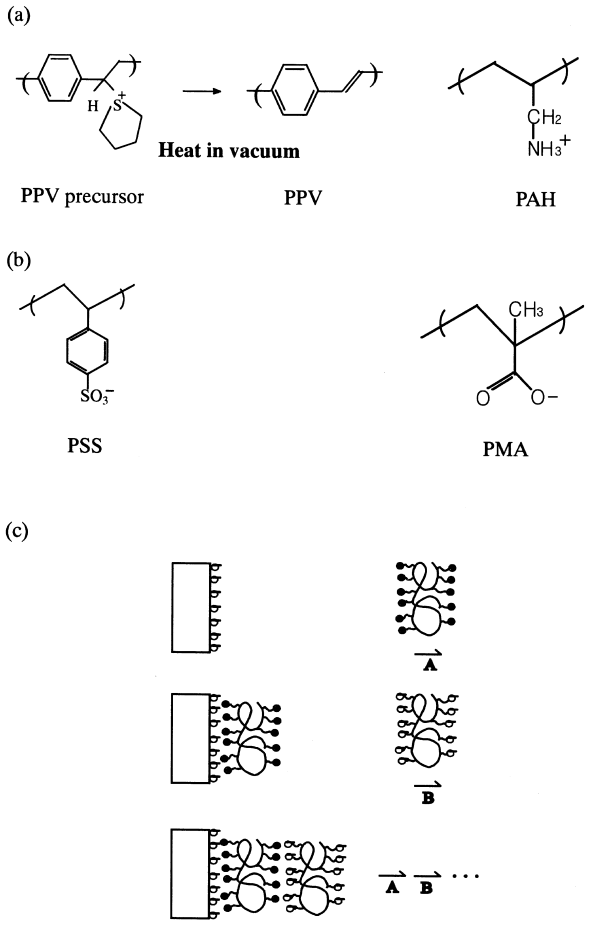

Fig. 1. Chemical structure of (a) positively charged and (b) negatively charged polymers. (c) A side view schematic depicting the buildup of multilayer assemblies by consecutive adsorption of anionic and cationic polyelectrolytes.

After each adsorption step, the surface of the self-assembled film was washed by dipping in Milli-Q water for 2 min and then blown dry with a stream of nitrogen gas. The washing and drying conditions for the fabrication of self-assembled film devices was identically applied to all the devices. All the films were then heated to 230°C for 1 h under vacuum (approx. 10^{-3} torr) for the PPV conversion. Fig. 1 shows the chemical structure of polymers used in this study and a schematic for the buildup of self-assembled multilayer films.

2.3. Measurement of current–light characteristics

LEDs based on the self-assembly were prepared in a similar fashion on indium tin oxide (ITO) coated glasses (obtained from Samsung Corning Co.). The thickness

of ITO layer is approximately 1850 Å and the sheet resistance is 10 ~ 20 Ω cm. The ITO substrates were cleaned by sonication in isopropyl alcohol for 1 h, followed by immersion in $H_2O/H_2O_2/NH_3$ (5:1:1) for 1 h. The preparation of self-assembled films on the ITO substrates is identical to the procedure adopted on the quartz glasses. After the thermal conversion of the PPV precursor to a conjugated form of PPV, aluminum counter electrode was evaporated onto the PPV multilayer films. The resulting film thickness was approximately 1500 ~ 2000 Å and the active area for light emission is 16 mm^2.

The current–voltage–light (I–V–L) characteristics were recorded on a Keithly 236 Source/Measure Unit for the V–I relationship and by a Newport SIS-SL photodiode for the V–L intensity correlation.

2.4. Measurement of film thickness

The quantity of material deposited at each adsorption step was deduced from its UV absorption spectrum, obtained by a Perkin-Elmer Lambda 4B UV/visible spectrophotometer. The film thickness was determined by X-ray reflectivity using a Cu K_α ($\lambda = 1.54$ Å) beam from a narrow line source of an 18-kW Rigaku Ru-300 rotating anode generator. An ellipsometer (Auto EL-II) was also employed for the thickness confirmation.

3. Results and discussion

Polyelectrolytes carrying a large amount of ions, in general, adsorb preferably onto an oppositely charged surface. It has previously been reported that the adsorption behavior depends strongly on the ionic strength of solution and therefore, the adsorbed amount and the thickness of polyelectrolyte films are drastically increased by the addition of NaCl salt to the solution [6,9]. Our current purpose is to control the device characteristics based on the ionic strength of a dipping solution. For a number of experiments, the ionic strength of the PSS solution was adjusted to be 0.0, 0.1, 0.5 and 1.0 M by adding NaCl: the corresponding samples are denoted as $F_{0.0}$, $F_{0.1}$, $F_{0.5}$ and $F_{1.0}$, respectively.

3.1. Film thickness determination

The film thickness of the multilayer assemblies is determined with X-ray reflectivity and optical ellipsometry before and after the thermal conversion. Fig. 2a shows the specular X-ray reflectivity spectra of a PPV/PSS multilayer assembly ($F_{0.0}$) on a quartz substrate before and after the thermal conversion. Symbols in Fig. 2a are the measured reflectivity data and solid lines are the reflectivity curves from fitting the experimental points to a theoretical film model [10]. Well-defined Kiessig fringes [11] due to the interference of beams reflected from the upper and lower interfaces are clearly observed up to a scattering angle 2θ of 2.8°. Fitting the specular X-ray reflectivity data to a theoretical model allows the precise determination of film thickness and surface roughness. The thickness results are summarized in Fig. 2b. The linear relationship between film thickness and number of bilayers shows that the bilayer thickness stays relatively uniform throughout the structure. The thickness of a bilayer consisting of a PPV precursor layer and a PSS layer is determined to be approximately 8 ± 2 Å. This number implies that the precursor and the conjugated polymers in the PPV/PSS bilayer lie flat parallel to the substrate. After thermal conversion, the bilayer thickness is slightly reduced to 6 ± 1 Å. We believe that the decrease in the total film thickness results from the spatial rearrangements of polymer chains after removal of sulphonium groups of the PPV precursor during the thermal conversion. The root-mean-square (RMS) roughness at the film/air interfaces are approximately

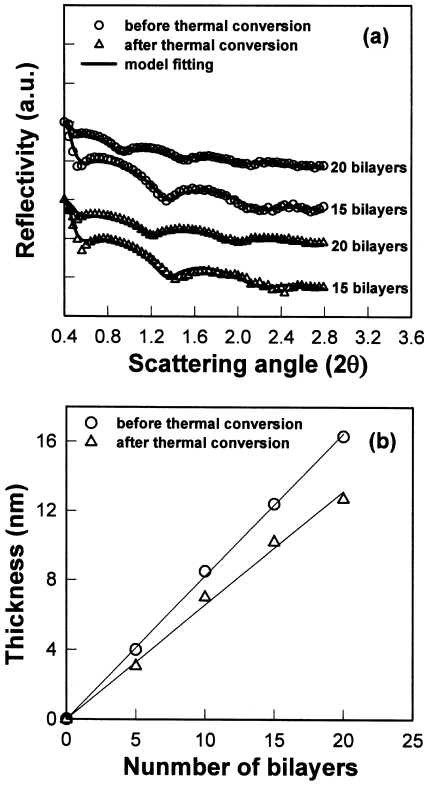

Fig. 2. (a) X-Ray reflectivity curves of 15 and 20 bilayers of a PPV/PSS film ($F_{0,0}$ sample); symbols (○, △) represent the actual reflectivity measured and solid line are the fitting of experimental data to a theoretical model. (b) The deduced film thickness as a function of number of bilayers deposited; ○ represents the measurement before thermal conversion, △ after thermal conversion. The thermal conversion was performed under vacuum at 230°C for 1 h.

9 ± 1 Å and 8 ± 1 Å before and after the thermal conversion, respectively.

By calibrating the thickness obtained with an ellipsometer to the thickness measured with X-ray reflectivity using $F_{0.0}$ sample, the thickness of 20 bilayer samples of $F_{0.0}$, $F_{0.1}$, $F_{0.5}$ and $F_{1.0}$ can directly be determined from ellipsometry.

3.2. Multilayer films

We have constructed multilayer film structures with alternating cationic and anionic polyelectrolyte layers. Cationic PPV precursor and anionic PSS were deposited on quartz substrates by using the layer-by-layer self-assembly method based on the electrostatic attraction between opposite charges.

Fig. 3 shows the UV absorbance per bilayer measured at 225 nm as a function of the number of deposited bilayers with different ionic strength values of PSS solution. Linear relationship is obtained between the adsorbed amount of polyelectrolytes and the number of layers, indicating the consistent film adsorption throughout the deposition process. The ionic strength of the dipping PSS solution is controlled with NaCl salt concentration. The effect of NaCl electrolyte concentration on the thickness of the deposited film is represented in Fig. 3. The thickness of each bilayer significantly increases upon the increase of NaCl concentration.

3.3. Current–light characteristics

To investigate the effect of added ionic salt in the self-assembled film on the quantum efficiency of EL devices, the L–I characteristics of the devices were measured. Fig. 4a shows the I–V and the L–V relationships obtained from ITO/(PPV/PSS)$_{20}$/Al EL devices as a function of NaCl concentration in the PSS solution. The total film thickness of the EL devices is 124 Å, 271 Å, 353 Å and 416 Å for $F_{0.0}$, $F_{0.1}$, $F_{0.5}$ and $F_{1.0}$, respectively. It was found from Fig. 4a that increasing the ionic strength of PSS solution yields the high operating voltage as well as the low and unstable light level of the EL devices. The absolute quantum efficiency in all devices was also found to be quite low ($< 10^{-5}$%). Since quantum efficiency of devices below 20 mA is also fluctuating, it is impertinent to compare the change in the quantum efficiency of devices with increasing the amount of ionic salts. Therefore, we have instead made the relative comparison of the device efficiency from the slope of L–I curve shown in Fig. 4b [12,13]: the larger the slope, the more efficient the device. In this case, the relative device efficiency of these (PPV/PSS)$_{20}$ EL devices decreases with the increase of ionic strength of the PSS solution and this trend is also reproducible in repeated I–V–L measurements. As a result, the added ionic salt in the self-assembled film decreases the device efficiency of light-emitting devices despite

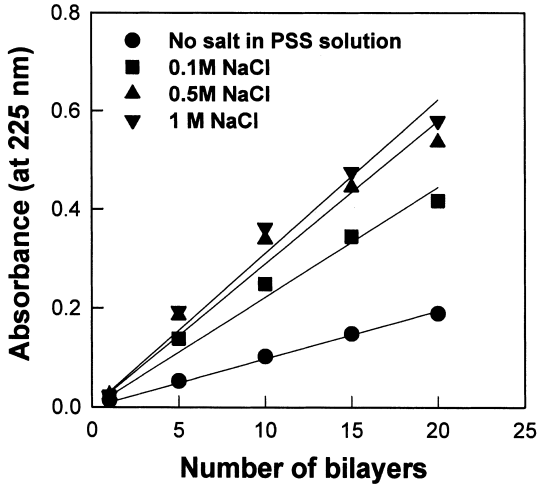

Fig. 3. UV absorbance (measured at 225 nm) as a function of number of PPV/PSS bilayers deposited onto quartz glasses with different NaCl ionic strengths of PSS solution.

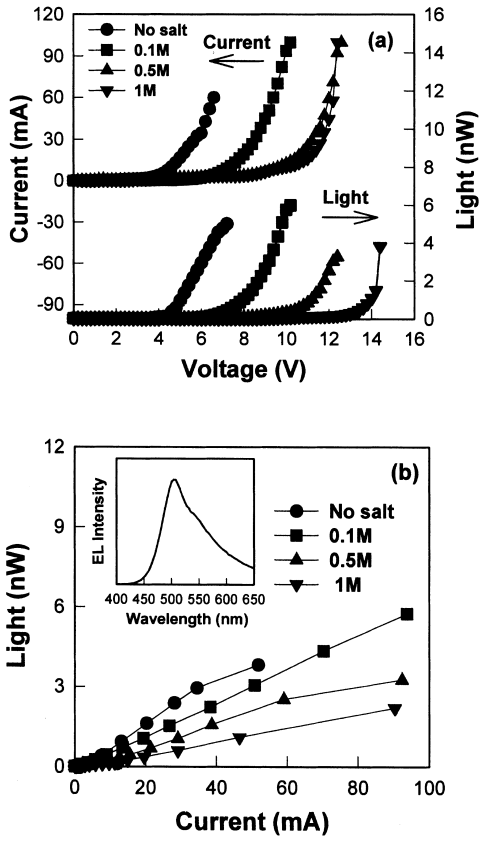

Fig. 4. (a) Current–light–voltage characteristics and (b) relative device efficiency of ITO/(PPV/PSS)$_{20}$/Al devices thermally converted at 230°C for 1 h with different ionic strength in PSS. The inset shows the EL spectrum of (PPV/PSS) film containing no ionic salt. Film thicknesses measured for the multilayer films are: 124 Å for 0 M, 271 Å for 0.1 M, 353 Å for 0.5 M and 416 Å for 1 M.

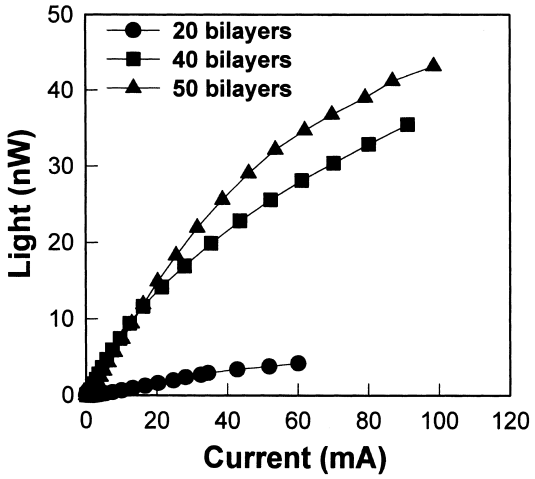

Fig. 5. Relative device efficiency of ITO/$(PPV/PSS)_n$/Al EL devices thermally converted at 230°C for 1 h with increasing (PPV/PSS) bilayers. No salt was added to the PSS solution. Film thicknesses of the multilayer films are: 124 Å for 20 bilayers, 252 Å for 40 bilayers and 320 Å for 50 bilayers.

the increased thickness of the total emitting layer, or more specifically, the increased recombination region of holes and electrons. The inset of Fig. 4b shows the EL spectrum of the ITO/$(PPV/PSS)_{20}$/Al device without ionic salt.

When the film thickness is increased without resorting to the increase in ionic salt concentration, the device efficiency of the EL device increases proportional to the film thickness. For instance, we increased the number of PPV/PSS bilayers to increase the total film thickness and this attempt resulted in the enhancement of quantum efficiency as shown in Fig. 5.

The focus of present study lies in understanding why the two different methods of increasing the total film thickness result in different performance in terms of quantum efficiency. Although we do not know the exact energy barrier height between the conjugated PPV and the insulating PSS layers since the energy levels of the self-assembled PPV films are slightly different from those of spin-casted PPV (i.e. 2.5 eV for HOMO and 5.1 eV for LUMO) [14] presumably due to the chain intermixing between the respective layers [15,16] and the restriction of conjugation bond growth of PPV by electrostatic attraction [6], this will help us better understand the EL mechanism and also provide us with guidelines for future EL device design. It is not too difficult to understand why the increase of total film thickness increase, for the case of increasing the number of bilayers, ends up with the enhancement of device efficiency as the current leakage would decrease and the recombination probability would also increase. It is, however, counter intuitive why the increase of the total film thickness would deteriorate the device efficiency of the device in the case of added salt experiments as shown in Fig. 4b. We believe that the decrease in device efficiency upon the increase of salt concentration is mainly attributed to the deposition of residual salt at the interface in direct contact between $(PPV/PSS)_{20}$ film and Al electrode. Although we cannot directly measure the amount of the residual salt as an impurity in the self-assembled films, we think that there is possibility that the residual salt at the (PPV/PSS) film/Al electrode interface induces the electronic interactions such as excited state quenching [17,18]. Ettedgui and his coworkers have reported that surface impurities can significantly alter the surface states of PPV/metal interfaces and the surface states at the interface can also be favorably modified with proper surface treatment [19]. In light of these reported results, it seems reasonable to conclude that these impurities formed near the Al electrode induce the inefficient electron injection from the Al electrode into the PPV/PSS films resulting in the non-radiative decay by way of polaron exciton quenching.

It has recently been reported that the quantum efficiency of EL devices was significantly improved by inserting a thin insulating layer at the interface between a conjugated polymer and an Al electrode [12,20]. The idea behind it is that the insulating layer acts as a hole blocking layer resulting in the exciton formation followed by the radiative decay of excitons near the conjugated polymer/insulator interface rather than at the conjugated polymer/Al electrode interface, thereby effectively eliminating the non-radiative quenching sites.

In order to confirm our hypothesis described above, we inserted the $(PAH/PMA)_1$ insulating layer of a 3.5-nm thickness between the (PPV/PSS) film and the Al electrode resulting in a multilayer structure of ITO/$(PPV/PSS)_{20}$/$(PAH/PMA)_1$/Al. The $(PPV/PSS)_{20}$ films were again prepared with different ionic strengths of PSS solution as described previously. Fig. 6

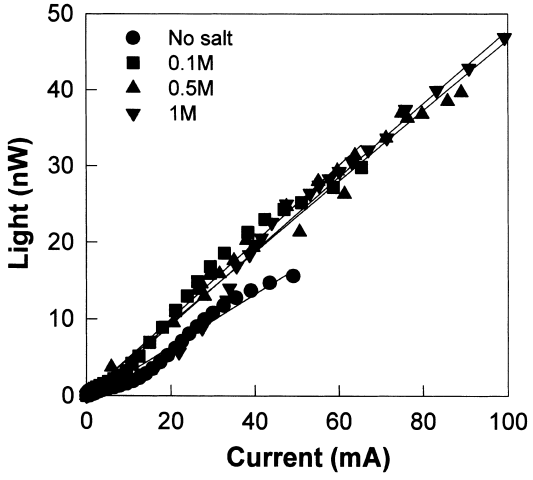

Fig. 6. Relative device efficiency of ITO/$(PPV/PSS)_{20}$/$(PAH/PMA)_1$/Al EL devices with different ionic strengths of PSS solution.

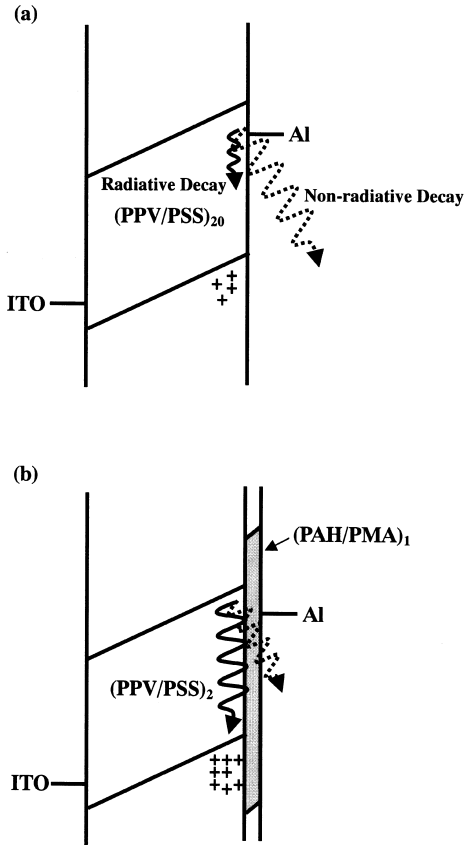

Fig. 7. Schematic energy band diagram illustrating the electroluminescence characteristics of self-assembled devices: (a) without an insulating layer; and (b) with (PAH/PMA) insulating layer.

shows the light–current characteristics measured on these devices. These devices secure stable and continuous light with increasing voltage and current compared with the devices containing no insulating layer. The most notable change is the improvement of device efficiency upon the increase of ionic salt concentration. In addition to the increase of net efficiency, it should also be noted that the relative quantum efficiency and the stability against high voltage are improved upon the total film thickness increase even for the cases where the film thickness increase was due to the added salt. All of these observations clearly indicate that residual salt in the multilayer self-assembled films induces defects for the non-radiative decay of excitons near the Al electrode and this effect deteriorates the device performance. In contrast, the inserted (PAH/PMA) insulating layer suppresses the defect formation at the (PPV/PSS) film/Al electrode interface. Without the defect formation induced by the residual salt, the increased recombination region leads to the increase in device efficiency.

This argument can also be explained on the basis of energy band diagram shown in Fig. 7. When the cathode is in direct contact with (PPV/PSS) films containing residual salts, many defects formed at the interface between the PPV/PSS bilayer and the cathode dominantly cause the non-radiative decay compared with the radiative decay as shown in Fig. 7a. However, the non-radiative decay upon the defect formation is significantly suppressed when a thin (PAH/PMA) insulating layer is inserted at the interface between the emitting layer and the cathode. Furthermore, the decrease of leakage current due to the hole blocking [21] at the interface between the (PPV/PSS) emitting layer and the insulating layer improves the net device efficiency as schematically shown in Fig. 7b. The insertion of a PAH/PMA insulating layer at the interface between a $(PPV/PSS)_{20}$ and an Al electrode improves the quantum efficiency presumably due to the shift of recombination region from the film/electrode interface to the film/insulator interface. With the addition of the insulating layer, the device efficiency significantly increases in proportion to the recombination region regardless of the fact that NaCl salt additive is used in a dipping solution in order to increase the total film thickness.

4. Conclusion

We prepared PPV/PSS alternating multilayer EL devices using a self-assembly technique and evaluated the film properties as well as device performance (i.e. in terms of relative quantum efficiency). The addition of NaCl salt to the PSS dipping solution significantly increases the adsorbed amount per bilayer but the relative quantum efficiency of $(PPV/PSS)_{20}$ EL devices decreases with the increase of the amount of NaCl. We attribute the decrease of the relative quantum efficiency, despite the increase in the recombination region, to the formation of unstable interface between the self-assembled film and the Al electrode due to residual salt in the self-assembled multilayer film. We successfully avoid the deleterious residual ionic salt effect by inserting a thin insulating layer in order to suppress the formation of unstable interface, resulting in the increase of the device efficiency of EL devices with the increased amount of NaCl salt in the dipping solution. We demonstrated in present system that the quantum efficiency of EL devices can be greatly improved by a combination of additive salt and proper layer arrangement of a multilayer device.

References

[1] P.K.H. Ho, M. Granstrom, R.H. Friend, N.C. Greenham, Adv. Mater. 10 (1998) 769.
[2] O. Onitsuka, A.C. Fou, M. Ferreira, B.R. Hsieh, M.F. Rubner, J. Appl. Phys. 80 (1996) 4067.
[3] G. Decher, J.-D. Hong, J. Schmitt, Thin Solid Films 210/211 (1992) 831.
[4] H. Hong, R. Steitz, S. Kirstein, D. Davidov, Adv. Mater. 10 (1998) 1104.
[5] M. Ferreira, J.H. Cheung, M.F. Rubner, Thin Solid Films 244 (1994) 806.

[6] J.-D. Hong, D. Kim, K. Char, J.I. Jin, Synth. Met. 84 (1997) 815.
[7] J.H. Cho, K. Char, D. Kim, S.-Y. Kim, J.-H. Hong, D.Y. Kim, K.B. Kim, Langmuir (in press).
[8] D.R. Gagnon, J.D. Capistran, F.E. Karasz, R.W. Lenz, S. Antoun, Polymer 28 (1987) 570.
[9] Y. Lvov, G. Decher, H. Mohwald, Langmuir 9 (1993) 481.
[10] A.M. Mayer, T.P. Russell, S.K. Satija, C.F. Majkrzak, Macromolecules 25 (1992) 6523.
[11] H. Kiessig, Ann. Phys. 10 (1931) 51.
[12] A.C. Fou, O. Onitsuka, M. Ferreira, M.F. Rubner, J. Appl. Phys. 79 (1996) 7501.
[13] O. Onitsuka, A.C. Fou, M. Ferreira, B.R. Hsieh, M.F. Rubner, J. Appl. Phys. 80 (1996) 4067.
[14] H. Mattoussi, L.H. Radzilowski, B.O. Dabbousi, D.E. Fogg, R.R. Schrock, E.L. Thomas, M.F. Rubner, M.G. Bawendi, J. Appl. Phys. 86 (1999) 4390.
[15] J. Schmitt, T. Grunewald, G. Decher, P.S. Pershan, K. Kjaer, M. Losche, Macromolecules 26 (1993) 7058.
[16] H. Hong, R. Steitz, S. Kirstein, D. Davidov, Adv. Mater. 10 (1998) 1104.
[17] A.R. Brown, D.D.C. Bradley, J.H. Burroughes, R.H. Friend, N.C. Greenham, P.L. Burn, A.B. Holmes, A. Kraft, Appl. Phys. Lett. 61 (1992) 2793.
[18] J. Birgerson, M. Fahlman, P. Broms, W.R. Salaneck, Synth. Met. 80 (1996) 125.
[19] E. Ettedgui, H. Razafitrimo, K.T. Park, Y. Gao, B.H. Hsieh, Surf. Interface Anal. 23 (1995) 89.
[20] H.M. Lee, K.H. Choi, D.H. Hwang, L.M. Do, T.H. Zyung, Appl. Phys. Lett. 72 (1998) 2382.
[21] Y.-E. Kim, H. Park, J.-J. Kim, Appl. Phys. Lett. 69 (1996) 599.